



# Badminton Flight Trajectory Location and Tracking Algorithm Based on Particle Filter

Zhiyong Huang<sup>1(✉)</sup> and Yuansheng Chen<sup>2</sup>

<sup>1</sup> Guangzhou Huashang Vocational College, Guangzhou 511300, China  
13560455687@163.com

<sup>2</sup> Guangzhou Huali College, Guangzhou 511325, China

**Abstract.** In order to meet the accuracy requirements of badminton robot, a badminton flight trajectory location and tracking algorithm based on particle filter is proposed. Collect badminton flight images for morphological and filtering processing. Using image features and matching to detect badminton flying targets. Predict the flight trajectory of a badminton ball considering its force situation. Using particle filter algorithm to determine the flight position of badminton, and through real-time updates, achieve the positioning and tracking of badminton flight trajectory. The experimental results show that the trajectory positioning and length tracking errors of the designed algorithm are 4.12 m and 0.13 m, respectively. The tracking update delay is only 7.6 s, and the tracking success rate is as high as 97%. The design method effectively solves the problems of large trajectory positioning tracking errors, low stability, and efficiency.

**Keywords:** Particle filter · Badminton · Flight path · Location tracking

## 1 Introduction

With the improvement of people's living standards, sports have been integrated into people's daily life. Among them, badminton is a sport suitable for all ages. In order to capture the dynamic path of badminton quickly and accurately, a badminton robot needs to be designed to track the high-speed badminton in real time. Target tracking can be defined as the process of obtaining the motion state information of the target continuously in the video sequence [1] based on the prior template information of the known target. Target tracking is a challenging technical difficulty in the field of computer vision. Target tracking technology is closely related to target detection and recognition technology. Generally, in practical engineering applications, it is necessary to detect the target of interest first, and then switch to automatic tracking mode after accurately capturing the target. During the tracking process, it constantly analyzes the information such as target shape, scale, and motion rules, and evaluates, classifies, and recognizes the target attributes. Target tracking technology plays an important role in both military and civilian fields.

After a long time of research, the current track location and tracking algorithm development is more mature, including: track location and tracking algorithm based on multi-sensor, track location and tracking algorithm based on dynamic Snake model, and track location and tracking algorithm based on network computing. The track location and tracking algorithm based on multi-sensor uses mobile robots as tracking targets, According to its kinematic model, analyze the key parameters of motion control in the trajectory tracking process, collect and fuse multi-sensor data, process the signals of each sensor respectively, and fuse the angle information on this basis, so as to reduce the positioning error. The fuzzy control method is studied to realize the application of fuzzy control in the trajectory tracking of mobile robots, and good positioning and tracking results are obtained. The track location and tracking algorithm based on dynamic Snake model combines KLT optical flow method, selects the strong feature points in the contour points obtained in the current frame to estimate the optical flow, takes the estimation result as the initial contour of the next frame Snake, and determines the target location and tracking results according to the contour features of the target. However, the above flight path location and tracking algorithm is still very complex and faces many challenges in the actual operation process, including: the information loss caused by the projection from the three-dimensional world to the two-dimensional image plane makes tracking difficult; Noise in the image itself; Tracking the light changes in the scene, mutual occlusion between objects, etc. Applying the traditional location and tracking algorithm to the location and tracking of badminton flight trajectory, there is an obvious problem of large location and tracking errors. Therefore, particle filter algorithm is introduced.

The so-called particle filter is to find a group of Random sample To approximate probability density function, using Sample mean Instead of integral operation system state Of Minimum variance estimation These samples are vividly called “particles”, so they are called particle filtering. The idea of particle filter is based on Monte Carlo method, which uses particle set to represent probability, and can be used in any form of state space model. Its core idea is to learn from Posterior probability It is a sequential importance sampling method to express the distribution of random state particles extracted from. The particle filter algorithm is used to optimize the location and tracking algorithm of badminton flight trajectory, in order to improve the location and tracking accuracy of badminton flight trajectory. Based on the above analysis, this article proposes a badminton flight trajectory localization and tracking algorithm based on particle filtering. Collect badminton flight images, preprocess the initial flight images through morphology and filtering to obtain the correct moving target. By using image features and matching, detect badminton flying targets, consider the force on the badminton, and predict the badminton flight trajectory. Using particle filter algorithm to determine the flight position of badminton, real-time updates are used to achieve badminton flight trajectory positioning and tracking, thereby improving the positioning and tracking accuracy of badminton flight trajectory.

## 2 Design of Badminton Flight Trajectory Location and Tracking Algorithm

### 2.1 Collecting Badminton Flight Images

Through stereo vision to identify and track badminton, reconstruct the three-dimensional information of badminton in the badminton court. This requires the visual system to cover the court completely and without blocking. At the same time, in order to find badminton earlier, the visual height is generally higher than the net height. The fixed focus industrial camera is selected as the stereo vision equipment. The measurement accuracy of the stereo vision equipment in the Z-axis direction is required to be:

$$c_Z = \frac{h^2}{d_{\text{optic axis}} * f} W_{xy} \tag{1}$$

Among them,  $h$  is the depth of field,  $d_{\text{optic axis}}$  and  $f$  are the optical axis distance and camera focal length,  $W_{xy}$  is the pixel size of the visual device [2]. The measurement accuracy  $c_X$  and  $c_Y$  of stereo vision equipment in the X-axis and Y-axis directions are:

$$c_X = c_Y = \frac{h}{f} W_{xy} \tag{2}$$

According to Formula 1 and Formula 2, the measurement error in the depth direction is proportional to the square of the measurement distance, and the measurement error in the X and Y directions is proportional to the measurement distance. Use the stereo vision equipment that meets the accuracy requirements to obtain the acquisition results of badminton flight images according to the representation principle in Fig. 1.

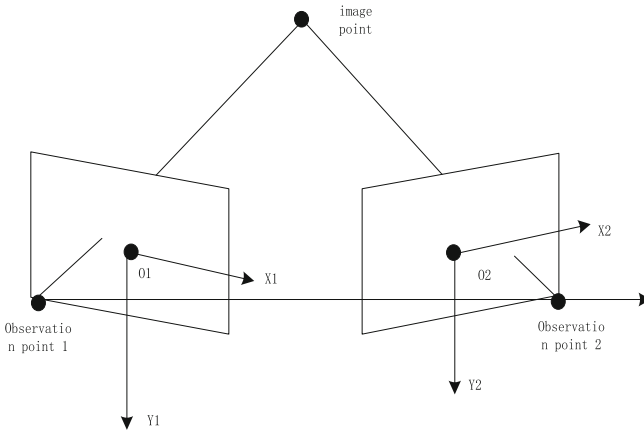


Fig. 1. Schematic diagram of badminton flight image acquisition

In order to avoid measurement distortion caused by wide-angle lens distortion during badminton flight image acquisition, a 100° field of view lens is selected. Set the image acquisition frequency, and get the image acquisition results at any time during the badminton flight.

## 2.2 Initial Badminton Flight Image Pre-processing

Generally, because the camera has shifted or rotated, the image background in the image sequence will produce motion, and the motion of the background will lead to the change of the coordinate system where the target is located. A series of operations against the target will produce errors, resulting in the final failure to obtain the moving target correctly. When this happens, in order to obtain the moving target in the image sequence using the frame difference method and other methods, it is necessary to first register the image sequence and convert it to the same coordinate system. This method is called global motion compensation [3, 4]. The essence of global motion compensation is to find the corresponding relationship between two adjacent images, and then convert the two images to the same coordinate system through this relationship. The main steps of the algorithm are described as follows: first, find the corresponding feature points in the two images, and then obtain the geometric transformation model between their position coordinates according to the position information of the two feature points in their respective images, so that other pixel points in the two images can be transformed into the same coordinate system through this transformation model. Then the image on the moving background can be further processed as the image on the fixed background. Morphological filtering uses the information of the image contained in the structure element to carry out logical operations on the corresponding area pixels, obtain new pixels after filtering, and constantly update the pixels in the image to achieve the purpose of changing the overall structure of the image. The morphological filtering processing results of the initial badminton flight image can be expressed as:

$$\begin{cases} A \odot B = \{z_{\text{corrosion}} | (B)_{z_{\text{corrosion}}} \subseteq A\} \\ A \oplus B = \{z_{\text{expansion}} | (B)_{z_{\text{expansion}}} \cap A \neq \emptyset\} \end{cases} \quad (3)$$

In the above formula,  $A$  and  $B$  they respectively represent the badminton flight image and structural elements initially collected,  $z_{\text{corrosion}}$  and  $z_{\text{expansion}}$  corresponds to the results of image erosion and expansion processing.  $(B)_{z_{\text{corrosion}}}$  and  $(B)_{z_{\text{expansion}}}$  are the corrosion and expansion treatment results of structural elements, respectively. Due to jitter, external light, wind and other factors in the image acquisition process, there will be some noise in the image generation process, which will reduce the image quality and have a negative impact on the further processing of later images. Therefore, image filtering algorithm is often used for image denoising. In order to ensure the image preprocessing effect, the processing method of combining mean filtering, Gaussian filtering and median filtering is adopted. The mean filtering is to replace the pixel value of each pixel in the local neighborhood of the original image with the mean value of all pixel values in the neighborhood. The process of mean filtering  $I_{\text{Mean filtering}}(x, y)$  can be quantified as:

$$I_{\text{Mean filtering}}(x, y) = \frac{1}{m} \sum I(x, y) \quad (4)$$

Among them,  $m$  refers to the number of pixels in the badminton flight image,  $I(x, y)$  represents the flying image of badminton. In addition, the basic principle of Gaussian filtering is that the weight value is selected according to the shape of the Gaussian function, and the median filtering is to assign the pixel value of the original image through

the processing of the template [5]. The process of Gaussian filtering  $I_{\text{Gaussian filter}}(x, y)$  and median filtering  $I_{\text{median filtering}}(x, y)$  is as follows:

$$\begin{cases} I_{\text{Gaussian filter}}(x, y) = \frac{1}{2\pi\chi^2} \exp \frac{-I(x+y)^2}{2\chi^2} \\ I_{\text{median filtering}}(x, y) = \text{med}\{I(x - m_x, y - m_y)\} \end{cases} \quad (5)$$

In Formula 5,  $\chi^2$  is the variance of image pixels,  $m_x$  and  $m_y$  respectively represents the number of pixels in the horizontal and vertical directions of the badminton flight image,  $\text{med}\{\}$  is the median calculation function. Repeat the above operations, filter all the pixels in the collected badminton flight images, and obtain the preprocessing results of the initial badminton flight images.

### 2.3 Detection of Badminton Flying Targets

The detection principle of badminton flying target is: according to the characteristics of badminton flying environment, realize the separation of foreground and background, and extract the features of foreground image. Through the matching of foreground image features and badminton features, determine whether there are badminton flying targets in the current image, and then obtain the detection results of badminton flying targets. Figure 2 shows the basic detection process of badminton flying targets.

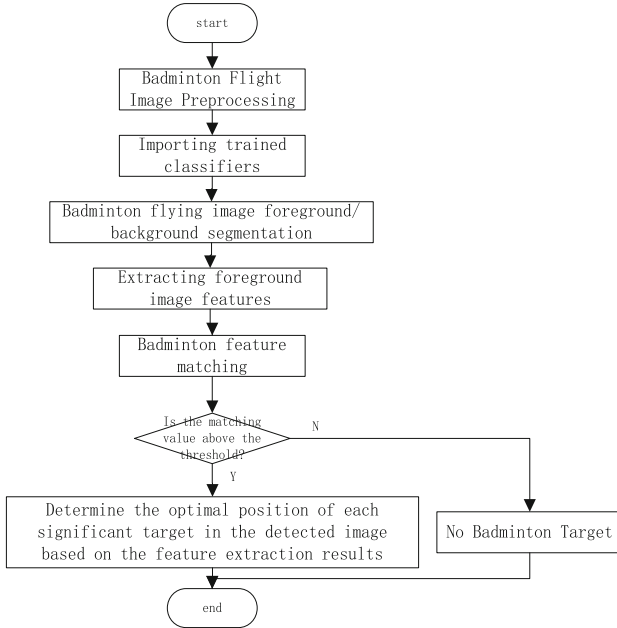


Fig. 2. Flow chart of badminton flying target detection

Let two single channel gray images of the same size for difference operation be  $I_1(x, y)$  and  $I_2(x, y)$ , the image after difference operation is  $I_{\text{prospect}}(x, y)$ , we can get:

$$I_{\text{prospect}}(x, y) = |I_2(x, y) - I_1(x, y)| \quad (6)$$

It can be seen from Formula 6 that the target can be enhanced by calculating the absolute value of the pixel difference at the corresponding position of the two images. There are light, wind and other interferences in the external environment, resulting in a lot of noise in the real scene. Therefore, in order to obtain a stable background, background modeling [6] is required. Mathematically, it can be realized through a single Gaussian model, in which the iterative process of the mean and covariance of image pixels represented by the model is:

$$\begin{cases} \mu_{t+1} = (1 - \omega)\mu_t + \omega I_t \\ A_{t+1} = (1 - \omega)A_t + \omega(I_t - \mu_t) \end{cases} \quad (7)$$

Among them,  $\omega$  is the experience threshold,  $A_t$  and  $A_{t+1}$  are  $t$  and  $t + 1$  covariance matrix of time,  $\mu_t$  and  $\mu_{t+1}$  are the pixel mean values of the badminton flight images at time  $t$  and  $t + 1$ , respectively. The background part of the image can be obtained by Formula 7, and the image difference can be performed by Formula 6 to realize the division of foreground and background. On this basis, color, contour, texture, gradient and other features are extracted from the foreground image in the image, and color features and gradient direction features are fused to generate a comprehensive histogram feature. The color histogram feature has little change in the case of plane rotation and partial occlusion, which is suitable for describing the target and is widely used. In order to reduce the influence of light changes during tracking, HSV color space [7, 8] is used. The kernel function representing spatial information is used to calculate the weighted histogram, which improves the robustness of the color histogram to describe the target features; The edge area may contain background, with small contribution and small weight allocation. Each channel of H and S components is assigned a quantization level of 8. Assume that the target state is  $(i, j)$  is the center,  $r$  is the radius, and the position of the pixel in the target area is  $X_i$ , then the normalized color histogram in the target area is:

$$Q_{\text{colour}} = \frac{\sum_{i=1}^m X_i f_{\text{Weight}}\left(\left\|\frac{1}{r}\right\|\right) f_{\text{delta}}[\varphi(X_i) - \lambda]}{\sum_{i=1}^m X_i f_{\text{Weight}}\left(\left\|\frac{1}{r}\right\|\right)} \quad (8)$$

Among them,  $f_{\text{Weight}}()$  and  $f_{\text{delta}}()$  are weight kernel function and delta function respectively,  $\varphi()$  represents the image of the color level index on the histogram,  $\lambda$  is the index of the color level in the histogram. Similarly, the extraction results of contour features, texture features, and gradient features can be obtained. Finally, the feature extraction results are fused and marked as  $Q$ . Match the image foreground image features with badminton standard features, and the matching results are as follows:

$$s = \frac{Q(t) \cdot Q_{\text{badminton}}}{\|Q(t)\| \cdot \|Q_{\text{badminton}}\|} \tag{9}$$

Among them,  $Q_{\text{badminton}}$  is a standard feature of badminton,  $Q(t)$  express  $t$  the feature extraction results [9] of badminton flight images were collected at all times. If the result of Formula 9 is higher than the threshold  $s_0$ , indicating that there is a badminton flying target in the current image, otherwise it is considered that there is no tracking target in the current image.

### 2.4 Predetermine Badminton Flight Path

Through the analysis of the real-time force on badminton, the basic trend of badminton flight trajectory is judged, and the prediction results of badminton flight trajectory are obtained. Figure 3 shows the stress of badminton in flight.

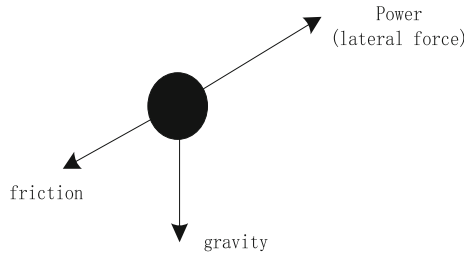


Fig. 3. Schematic diagram of force analysis of flying badminton

Badminton is mainly affected by aerodynamics and gravity during flight. Gravity is always vertically downward. Aerodynamics can be divided into three components, including the resistance along the badminton flight path, the lift that prevents the badminton from falling, and the lateral force that makes the badminton track yaw sideways [10]. The aerodynamic force on the badminton is in direct proportion to the maximum cross-sectional area of the badminton and the incoming flow pressure. The following three equations can be obtained:

$$\begin{cases} X = \kappa_{\text{resistance}} P \cdot S \\ Y = \kappa_{\text{lift}} P \cdot S \\ Z = \kappa_{\text{lateral force}} P \cdot S \end{cases} \tag{10}$$

Among them,  $\kappa_{\text{resistance}}$ ,  $\kappa_{\text{lift}}$  and  $\kappa_{\text{lateral force}}$  represent drag coefficient, lift coefficient and lateral force coefficient respectively, and the above coefficients are dimensionless proportional coefficients.  $P$  represents the actual flow pressure,  $S$  represents the maximum cross-sectional area of badminton. When the badminton flies at a certain initial speed in the air, the badminton will hit the air, and the air will make the badminton blades converge to the axis, and part of the air will also be compressed, so that the air

pressure at the front end of the badminton cork will increase, and the air will produce a force opposite to the movement direction of the badminton, which is called air resistance. Generally speaking, badminton can be divided into two parts, the front part composed of cork, which gathers most of the weight of the badminton and the skirt part composed of 16 pieces of fur. The weight is light, but it will produce air resistance during flight. Based on this mass arrangement, the gravity gravity center of the badminton should be located at the head of the badminton. The badminton skirt forms a large wind resistance plane in the badminton flight direction. Compared with the ball holder, it will suffer greater air resistance, so the force application point of air resistance is concentrated at the tail of the badminton. Considering the force characteristics of badminton, the prediction results of badminton flight trajectory are obtained.

## 2.5 Using Particle Filter Algorithm to Determine Badminton Flight Position

Combined with the prediction results of badminton flight trajectory, the accurate flight position of badminton in the image is determined using particle filter algorithm. Figure 4 shows the operation principle of particle filter algorithm.

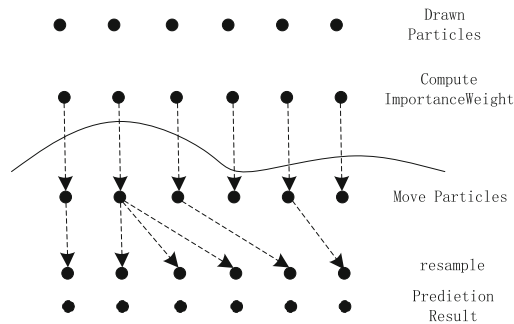


Fig. 4. Schematic diagram of particle filter algorithm

Following the principle shown in Fig. 4, the particle filter algorithm is executed through the steps shown in Fig. 5.

In the actual badminton flight positioning process, first initialize the particles in the badminton flight environment, and get the initial probability density distribution  $n_{\text{particle}}$  particle set of points, initialize all particle weights to:

$$\varpi_0 = \frac{1}{n_{\text{particle}}} \quad (11)$$

At time  $k$ , the dynamic model of object motion is used to predict the particle state at time  $k$  and generate the particle set at time  $k$  [11]. Formula 12 is used to update the weight of each particle in the particle set at time  $k$ :

$$\varpi_k = \varpi_0 \rho(x_k^i) \quad (12)$$

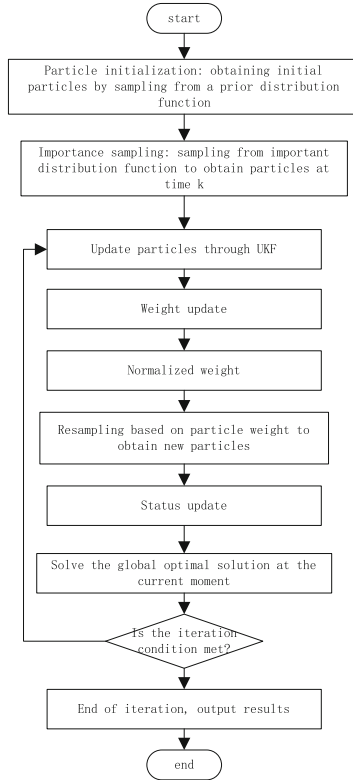


Fig. 5. Operation flow chart of particle filter algorithm

Among them,  $\rho()$  represents the probability density distribution of particles,  $x_k^i$  represents the state variable of the particle at time  $k$ . The effective sampling scale is defined as:

$$L_{eff} = \frac{1}{n_{\text{particle}} \sum_{k=1} \varpi_k} \quad (13)$$

If  $L_{eff}$  is less than the threshold value, resampling will be performed. In the process of iteration, the weight of some particles will become smaller and smaller. These particles do not help state estimation much. Instead, they will occupy a lot of computing resources. Therefore, it is necessary to evaluate the weight of all particles to resample particles. That is, the particles with large weight value are copied and the particles with small weight value are reduced, and the small weight particles are replaced by the new sample sequence with the same weight value. Because the residual resampling algorithm has relatively high calculation efficiency and small calculation variance, the residual resampling algorithm [12] is adopted. Repeat the above operations to obtain the global optimal solution at the current time. After the iteration conditions are met, the

output particle filter result is the positioning result of the badminton flight path, marked as  $(u(t), v(t))$ .

## 2.6 Realize Badminton Flight Track Positioning and Tracking

According to the above method, the badminton flight track positioning results at each time are fused to obtain the positioning and tracking results of the badminton flight track. The tracking results can be quantified as:

$$G = \sum_{t=1}^T (u(t), v(t)) \quad (14)$$

Among them,  $T$  is the flight time of badminton. Finally, the positioning and tracking results of badminton flight trajectory are visualized and marked with real-time flight trajectory position information to complete the positioning and tracking of badminton trajectory.

## 3 Experimental Analysis of Track Location and Tracking Performance Test

For the purpose of verifying the trajectory location and tracking accuracy of the badminton flight trajectory location and tracking algorithm based on particle filter, a performance test experiment was designed by combining white box and comparison. The basic principle of this experiment is to install a micro position sensor on the badminton equipment to be located and tracked, obtain the actual value of the real-time position of the badminton, and use this as the comparison standard to judge the accuracy of the location and tracking results of the badminton flight trajectory based on particle filter. In the process of badminton flight, start the location tracking algorithm of optimal design, get the corresponding output results, compare with the actual values obtained, and get the test results that reflect the tracking accuracy of the optimal design algorithm. The principle of comparative testing is to compare the accuracy test results of the design algorithm with the accuracy performance of the traditional algorithm, reflecting the advantages of the design method in performance.

### 3.1 Choose Badminton and Its Flight Environment

In this experiment, the standard badminton is selected as the target of location and tracking. The length of the standard badminton is between 64 mm and 70 mm. For the same badminton, all the hair pieces are the same length. The top opening of the badminton is arranged in a circular pattern, and the opening diameter is between 58 mm and 68 mm. The smaller the diameter of the badminton, the smaller the flight resistance in the air, the farther the flight distance, and the heavier the ball head will produce the same situation, and vice versa. The badminton feather flying at high speed in the air will be subjected to lateral force, which will lead to the spin of the badminton. The faster the spin speed is, the slower the flight speed of the badminton will be. On the

contrary, the faster the flight speed of the badminton will be. Generally, it is better to keep the spin speed at 370–400 rpm. The standard badminton court is selected as the flight environment of badminton, as shown in Fig. 6.



**Fig. 6.** Actual View of Badminton Flight Field

The standard badminton court is arranged in a rectangle. The sidelines of the court are drawn with white paint with a width of 40 mm. The sidelines are divided into singles and doubles. The width of the singles sideline is 5.18 m, the length is 13.40 m, and the width of the doubles sideline is 6.10 m, the length is 13.40 m. The middle height of the court is 1.524 m. The court is divided into two halves. Players from both sides hit the ball in two halves of the net. According to the regulations of international competitions, the height of the standard badminton court should be at least 9 m. There should be no interfering objects in the entire three-dimensional space where the badminton court is located, so as to ensure that the feather apparatus can fly in the air without interference. The color of the court wall should be dark, and there should be no reflectors or reflective surfaces, so as to avoid interference to athletes. The wind speed in the court should not be greater than 0.2 m/s. Before the experiment, a micro position sensor with a weight of no more than 1g shall be embedded inside the badminton court, and the real-time collected data of the sensor shall be transmitted to the host computer by using the wireless communication network covered inside the badminton court.

### 3.2 Configure the Flight Path Location and Tracking Algorithm Operating Environment

In order to make the platform and experimental data more accurate, the Intel model i74790 central processor with better hardware facilities is selected. The size of the memory card is 8 GB, which can store the data to be used. The hard disk requirements are relatively high, and 36 GB can be selected to avoid insufficient memory. The network card is set within the range of 1000 mb/s. In order to realize the visual output and measurement of the badminton flight track positioning and tracking results, SONY FCB-EX480CP

series new high pixel DSP integrated color analog camera is adopted. It has super light sensitivity and intelligent automatic night vision function, and can remotely set all camera parameters without manual operation, The camera image parameters can be adjusted in time according to the effect of the monitor image to present the image optimization. The minimum illumination of the camera is color 0.7 lx, and the power consumption range is [1.5 W, 2.5 W]. The MV-200 industrial image acquisition card is used as the image acquisition card. This industrial image acquisition card can capture high-precision images in real time, with stable hardware structure design and underlying functions, good hardware compatibility, and can work stably and reliably in a harsh working environment. MV-200 industrial image acquisition card can capture images with high definition, high resolution and high fidelity. In terms of software environment, software development is carried out under the Windows operating system, and the integrated development environment is Visual Studio 2013.

### 3.3 Input Operation Parameters of Particle Filter Algorithm

In order to meet the call requirements of the badminton flight path location and tracking algorithm to the particle filter algorithm in the running process, the relevant operation coefficient of the particle filter algorithm is set. Set the total number of initial particles to 200, the movement time to 15 s, and assume that one action is taken every second. In addition, the size of the sports field is consistent with the size of the badminton flight field selected.

### 3.4 Describe the Performance Test Process

This experiment was conducted in the singles scene, and the number of target shuttles tracked in the scene was 1. Athletes with more than 3 years of badminton experience were selected as the athletes for this experiment to ensure that the three movements of high distance ball, flat shot and pick ball were completed in badminton. With the support of sensors, the actual position information of badminton was obtained, as shown in Table 1.

Take the data in Table 1 as the actual position data of badminton flight track. In the configured experimental environment, the optimized badminton flight path location and tracking algorithm based on particle filter is converted into program code that can be run directly by the computer by using development tools, and the set running parameters of particle filter algorithm are input into it. Start the positioning and tracking procedure before the start of badminton movement, and get the corresponding flight path positioning and tracking results with the badminton movement, as shown in Fig. 7.

Therefore, the tracking position information of badminton flight track at any time can be obtained. In order to reflect the performance advantages of the design algorithm, the traditional track location and tracking algorithm based on multi-sensor and the track location and tracking algorithm based on dynamic Snake model are set as the experimental comparison algorithm. The development and operation of the comparison algorithm are completed according to the above process, and the corresponding flight track location and tracking results are obtained.

**Table 1.** Information of actual position of badminton flight track

Time/s	Lob		Flat shot		Pick the ball	
	x	y	x	y	x	y
1	10	1.6	10	1.1	10	0.6
2	15	1.8	15	1.1	10	0.8
3	20	2.0	20	1.1	12	1.0
4	25	2.2	25	1.1	15	1.6
5	30	2.5	30	1.1	20	1.7
6	35	2.3	35	1.2	25	1.8
7	40	2.2	40	1.2	30	1.9
8	45	2.0	45	1.1	35	2.0
9	50	1.8	50	1.1	40	2.2
10	55	1.6	55	1.1	45	2.4

### 3.5 Setting Performance Test Indicators for Track Positioning and Tracking

According to the purpose of the experiment, the tracking performance of the algorithm is reflected from the tracking accuracy and tracking timeliness of the track location. The test indicators of the tracking accuracy are tracking error and track length error. The numerical results are as follows:

$$\varepsilon = \sum_{t=1}^{t_{\text{experiment}}} |x_{\text{track}}(t) - x_{\text{reality}}(t)| + |y_{\text{track}}(t) - y_{\text{reality}}(t)| \tag{15}$$

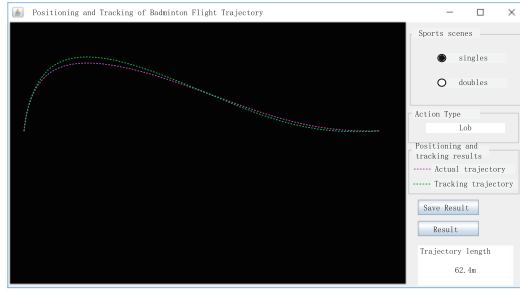
In the above formula,  $(x_{\text{track}}(t), y_{\text{track}}(t))$  and  $(x_{\text{reality}}(t), y_{\text{reality}}(t))$  represent the badminton position tracking result and actual position coordinates respectively. The test results of badminton flight path length tracking error are as follows:

$$\varepsilon_l = |l_{\text{track}} - l_{\text{reality}}| \tag{16}$$

Among them,  $l_{\text{track}}$  and  $l_{\text{reality}}$  are the tracking value and the actual value of the badminton flight path length. In addition, the test index of track tracking timeliness is tracking update delay, and its numerical result is:

$$\Delta t = t_{\text{out}} - t_{\text{sense}} \tag{17}$$

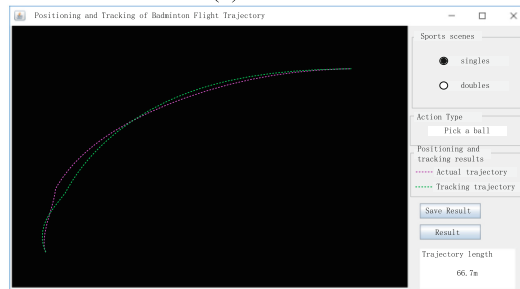
where,  $t_{\text{out}}$  indicates the output time of badminton flight track positioning and tracking results,  $t_{\text{sense}}$  the time of data generation is sensed by the built-in sensor for badminton. Finally, the smaller the tracking error and track length error are, which proves that the higher the tracking accuracy of the corresponding algorithm is, the smaller the tracking update delay is, which indicates that the better the track tracking timeliness is.



(a) Lob



(b) Flat shot



(c) Pick the ball

**Fig. 7.** Badminton Flight Path Positioning and Tracking Results

### 3.6 Performance Test Results and Analysis

Through the statistics of relevant data and the calculation of Formula 15, the test results of badminton flight track positioning and tracking error are obtained, as shown in Fig. 8.

It can be seen intuitively from Fig. 8 that the tracking error of the optimized design algorithm is smaller than that of the traditional positioning and tracking algorithm. Because the design method collects badminton flight images and preprocesses the initial flight images through morphology and filtering, effectively reducing the positioning and tracking error of badminton flight trajectory. In addition, the test results of track length error are shown in Table 2.

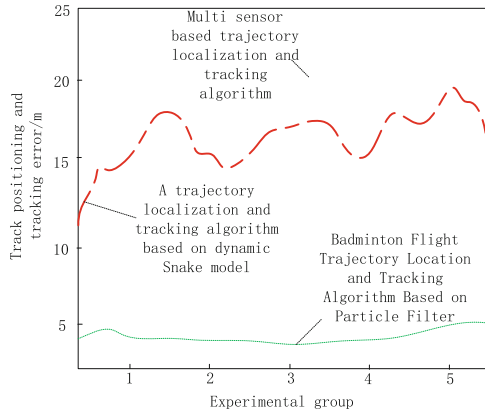


**Fig. 8.** Test results of badminton flight trajectory positioning and tracking errors using different methods

**Table 2.** Test Data Table for Length Error of Badminton Flight Trajectory by Different Methods

Experiment No	Actual length of badminton flight path/m	Multi sensor based track location and tracking algorithm output track length/m	Track location and tracking algorithm based on dynamic Snake model output track length/m	Badminton flight trajectory location and tracking algorithm based on particle filter output trajectory length/m
1	62.4	62.9	62.0	62.3
2	56.2	56.9	56.8	56.0
3	66.7	65.8	66.2	66.5
4	61.8	61.2	61.4	61.7
5	56.8	56.0	56.3	56.7
6	66.5	65.7	66.1	66.4

By substituting the data in Table 2 into Formula 16, it is calculated that the average track length tracking error of the two comparison algorithms is 0.72 m and 0.47 m respectively, and the average track length tracking error of the badminton flight track location and tracking algorithm based on particle filter is 0.13 m. In addition, the test results of track tracking timeliness are obtained through the calculation of Formula 17, as shown in Fig. 9.

As can be seen from Fig. 9, the average tracking update delay of the two comparison algorithms is 16.8 s and 17.2 s respectively, while the average tracking update delay of the badminton flight path location and tracking algorithm based on particle filter optimized design is 7.6 s.

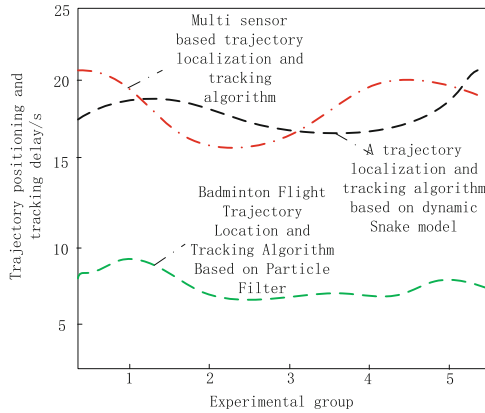


**Fig. 9.** Comparison results of time-effectiveness testing for badminton flight trajectory positioning and tracking using different methods

In order to verify the stability of badminton flight trajectory positioning and tracking in the design method, the success rate of tracking is used as an evaluation indicator. The higher the value, the higher the stability of badminton flight trajectory positioning and tracking in the method. Three methods were used for comparison, and the success rates of badminton flight trajectory localization and tracking using different methods are shown in Table 3.

**Table 3.** Success rate of badminton flight trajectory localization and tracking using different methods

Experiment No	Tracking success rate of trajectory positioning and tracking algorithm based on multiple sensors/%	Tracking success rate of trajectory positioning and tracking algorithm based on dynamic Snake model/%	Tracking success rate of badminton flight trajectory localization and tracking algorithm based on particle filter/%
1	92.0	89.3	98.9
2	91.8	87.0	96.7
3	90.2	86.5	95.8
4	91.4	88.7	97.2
5	92.3	86.7	96.5

According to Table 3, when the experimental number is 5, the tracking success rates of the multi-sensor based trajectory positioning and tracking algorithm and the dynamic Snake model based trajectory positioning and tracking algorithm are 91.5% and 87.6%, respectively. The tracking success rate of the badminton flight trajectory localization and tracking algorithm based on particle filtering is as high as 97%. From this, it can be

seen that the particle filter based badminton flight trajectory localization and tracking algorithm has high stability.

## 4 Conclusion

With the development of computer image processing technology and the advent of camera timely return visit system, visual tracking and detection technology has become increasingly mature, making target tracking and monitoring not only applied to artificial intelligence and other fields, but also launched a new chapter in sports. In sports, for the detection of balls, especially for the sphere moving in the air, because of its fast motion speed, ordinary cameras can not track its motion state in real time for the rapid movement of the sphere, and the image capture during the movement of the sphere will also have drag. The optimized badminton flight trajectory location and tracking algorithm based on particle filter effectively solves the problems existing in the traditional tracking algorithm, and realizes the accurate location and tracking of badminton flight trajectory. The experimental results show that the optimized design algorithm has good effectiveness and feasibility.

## References

1. Song, D., Gan, W., Yao, P., et al.: Guidance and control of autonomous surface underwater vehicles for target tracking in ocean environment by deep reinforcement learning. *Ocean Eng.* **250**, 110947 (2022)
2. Zuo, R., Li, Y., Lv, M., et al.: Realization of trajectory precise tracking for hypersonic flight vehicles with prescribed performances. *Aerosp. Sci. Technol.* **111**(2), 106554 (2021)
3. Lv, Z., Li, F., Qiu, X., et al.: Effects of motion compensation residual error and polarization distortion on UAV-borne PolInSAR. *Remote Sens.* **13**(4), 618 (2021)
4. Gishkori, S., Daniel, L., Gashinova, M., et al.: Imaging moving targets for a forward scanning SAR without radar motion compensation. *Signal Process.* **185**, 108110 (2021)
5. Pereira, S.C., Conde, E.R., Luz-de-Almeida, L.A., et al.: A power-line communication system employing median filtering for power control enhancement of wind generators. *Int. J. Commun. Syst.* **35**(12), e5203 (2022)
6. Wang, X.-W., Peng, H.-J., Liu, J., Dong, X.-Z., Zhao, X.-D., Lu, C.: Optimal control based coordinated taxiing path planning and tracking for multiple carrier aircraft on flight deck. *Defence Technol.* **18**(2), 238–248 (2022)
7. Lv, C., Li, J., Kou, Q., et al.: Stereo matching algorithm based on HSV color space and improved census transform. *Math. Probl. Eng.* **2021**, 1–17 (2021)
8. Waldamichael, F.G., Debelee, T.G., Ayano, Y.M.: Coffee disease detection using a robust HSV color-based segmentation and transfer learning for use on smartphones. *Int. J. Intell. Syst.* **37**(8), 4967–4993 (2022)
9. Dong, C., Guo, Z., Chen, X.: Robust trajectory planning for hypersonic glide vehicle with parametric uncertainties. *Math. Probl. Eng.* **2021**(5), 1–19 (2021)
10. Wang, B., Zhang, Y., Zhang, W.: Integrated path planning and trajectory tracking control for quadrotor UAVs with obstacle avoidance in the presence of environmental and systematic uncertainties: Theory and experiment. *Aerospace Sci. Technol.* **120**, 107277 (2022)
11. Buelta, A., Olivares, A., Staffetti, E., et al.: A gaussian process iterative learning control for aircraft trajectory tracking. *IEEE Trans. Aerospace Electron. Syst.* **57** (2021)
12. Cardoso, D.N., Esteban, S., Raffo, G.V.: A new robust adaptive mixing control for trajectory tracking with improved forward flight of a tilt-rotor UAV. *ISA Trans.* **2021**(110-), 110 (2021)